A&A 516, L10 (2010)
DOI: 10.1051/0004-6361/201014792

Astronomy & Astrophysics

Letter to the Editor

Thermal rotational lightcurve of dwarf-planet (1) Ceres at 235 GHz with the Submillimeter Array

A. Moullet[1], M. Gurwell[1], and B. Carry[2,3]

[1] Harvard-Smithsonian Center for Astrophysics, Cambridge MA-02138, USA
e-mail: amoullet@cfa.harvard.edu
[2] LESIA - Observatoire de Paris, 5 place J. Janssen, 92195 Meudon Cedex, France
[3] Université Paris 7 Denis-Diderot, 5 rue Thomas Mann, 75205 Paris Cedex, France

Received 14 April 2010 / Accepted 21 May 2010

ABSTRACT

Context. Previously published measurements of the millimeter-wave thermal rotational lightcurve of dwarf-planet (1) Ceres show incompatible results, proposing peak-to-peak lightcurve amplitudes during the ~9 h rotation period of either 4% or 50%, the latter being difficult to explain physically.
Aims. Better calibrated measurements are necessary to firmly assess the behavior of Ceres' thermal lightcurve, and to relate possible brightness temperature variations to the distribution of local surface properties such as bolometric albedo and emissivity.
Methods. One partial lightcurve of 6.5 h was obtained with the Submillimeter Array (Hawaii) in subcompact configuration at 235 GHz in January 2009, providing better absolute and relative calibration than the previously used single-dish facilities.
Results. The observed disk-averaged lightcurve is compatible with no variation over the measurement window, and has an upper limit of 3% on its amplitude.
Conclusions. The results obtained rule out the possibility of extreme brightness temperature variations, and the upper limit on the lightcurve amplitude could be physically realized by a combination of albedo distribution and realistic ground emissivity variations.

Key words. minor planets, asteroids: individual: Ceres

1. Introduction

The dwarf-planet (1) Ceres was the first asteroid to be discovered and the largest in size, but its low contrast visible and near-infrared (NIR) spectra have made it difficult to constrain the surface composition. Recently, spatially resolved maps in the visible (Li et al. 2006) and in the NIR (Carry et al. 2008) revealed a relatively homogeneous surface with features displaying albedo variations of only 4–6%.

It is also possible to indirectly map Ceres' surface properties by measuring disk-averaged brightness variations during its rotation (~9.1 h, Tedesco et al. 1983; Chamberlain et al. 2007). Because the shape of Ceres is close to an oblate spheroid (Thomas et al. 2005; Carry et al. 2008), those variations are uniquely related to surface properties such as albedo and, at thermal wavelengths, emissivity and thermal inertia. Most V-band lightcurves revealed amplitudes up to 4% (Tedesco et al. 1983; Li et al. 2006), which can be explained by relatively small albedo variations, as those measured by Li et al. (2006) and Carry et al. (2008), while the 3 μm lightcurve from Rivkin & Volquardsen (2010) ruled out disk-averaged albedo variations higher than 5% at that wavelength.

Millimeter-wave thermal lightcurves obtained from single-dish facilities, which mostly sound the thermal emission from ground layers located a few centimeters below the surface, showed significantly different behaviors : a maximum lightcurve amplitude of only 4% was observed at 250 GHz (Altenhoff et al. 1996), while at 345 GHz lightcurve amplitudes of up to 50% were reported (Chamberlain et al. 2009). The latter was interpreted as the result of very high emissivity and/or temperature variations. These would be linked to variations over large areas of soil properties such as roughness, absorption coefficient, refractive index or thermal inertia, which are difficult to explain physically. Moreover, since the depth of the sounded soil layers is typically a few tens of wavelengths, 250 GHz observations sound at most 1 cm deeper than 345 GHz observations, while still showing some contribution from upper layers. In the context of equilibrium thermal models, even with a strong variation of material composition with depth, this difference in observing frequency cannot explain such different behavior in the lightcurves, therefore the two results seem inconsistent.

In this context, the project presented here consists in obtaining a thermal rotational lightcurve at 235 GHz with the Submillimeter Array (SMA). The use of an interferometric facility allows a better sky contribution filtering than single-dish facilities, which in turn leads to a better absolute and relative calibration of the flux, and then a finer determination of intrinsic disk-averaged brightness temperature variations. Results are interpreted in terms of the surface properties distribution.

2. Observations

Ceres was observed during a 6.5 h track on 2009 January 28, sampling over 70% of the ~9.1 h long rotation curve, which is sufficient to display its complete surface. The array, consisting of 8 antennas of 6 m diameter located on Mauna Kea (Hawaii), was in its subcompact configuration, offering 28 baselines going from 9.5 m to 69 m. The low frequency receivers covered the 229.15-231.15 GHz frequency range in the lower side band

Table 1. Coordinates of the sources observed during the track and measured fluxes at 235 GHz.

Source	RA (hh:mm:ss)	Dec (°:′:″)	Max. elevation (°)	Flux (Jy)
Ceres	11:20:10	+20:38:59	87	3.30
Titan	11:30:31	+05:30:41	77	1.73
1159+292	11:59:31	+29:14:43	81	1.66
1043+241	10:43:09	+24:08:35	86	0.48

(LSB) and 239.15–241.15 GHz in the upper side band (USB), providing a synthesized beam of 4″ × 3.5″ at Ceres' 20° declination. Because Ceres' apparent size at the moment of the observations was only 0.76″, the dilution of Ceres in the synthesized beam was low enough for us to consider it as a point source, which also means that only disk-averaged measurements can be derived .

To ensure the best sampling of the rotation curve, Ceres was repeatedly observed every 24 min during a 6 min integration. Because the purpose of this track was to accurately assess temporal emission variations of Ceres, the main difficulty was to distinguish instrumental gain variations from the source's intrinsic emission variation. Observations were then performed to allow the best relative calibration of phase and amplitude with respect to time, hour-angle and elevation. To do that, gain calibrator quasars 1159+292 and 1043+241 were each observed during a 6 min-long integration in between each Ceres integration. These quasars were chosen for their proximity to Ceres on sky (see Table 1), so they could reveal and help to correct potential hour-angle and elevation-dependent gain variations. Their observation was followed by a 6 min integration on Titan, whose brightness temperature is known at a 5% precision level (and does not present temporal variations), and was hence used both as an absolute flux scale calibrator reference and an amplitude gain calibrator. To keep pointing errors under ∼5° (corresponding to a loss of ∼1% in signal strength), measurements of the pointing of each dish were obtained on Saturn and corrected approximately every two hours.

The quality of the sky was good with an opacity of only 0.15 (at the standard reporting frequency of 225 GHz), allowing the system temperature to be below 130 K most of the time. Spectral instrumental effects, which if uncorrected reduce the signal-to-noise ratio (SNR) of our continuum measurements, were calibrated using observations of generally flat-spectrum sources including Saturn, 3c273 and 1159+292, and Ceres itself. This passband calibration produces spectral gain corrections that are independent of time during a track, providing improved sensitivity for the full continuum bandwidth of 2 GHz in each sideband. The calibration of phase gain variations with time was done by self-calibration on all sources, using a point model for quasars and a disk model for Ceres and Titan. A series of amplitude gain corrections versus time and elevation was derived from both reference quasars, and applied to all the data.

Absolute flux calibration was applied with the USB observations of Titan near 240 GHz as a reference. The disk-averaged brightness temperature was assumed to be 77.4 K (modeled according to Gurwell & Muhleman (1995, 2000), and Gurwell (2004)), resulting in a flux density of 1.59 Jy in the USB. Again using the above models, we calculated the band-averaged flux density to be 1.95 Jy in the LSB due to CO emission in the stratosphere.

Measurements of each source flux density were then performed by fitting the visibility data on 6-min long sub-intervals,

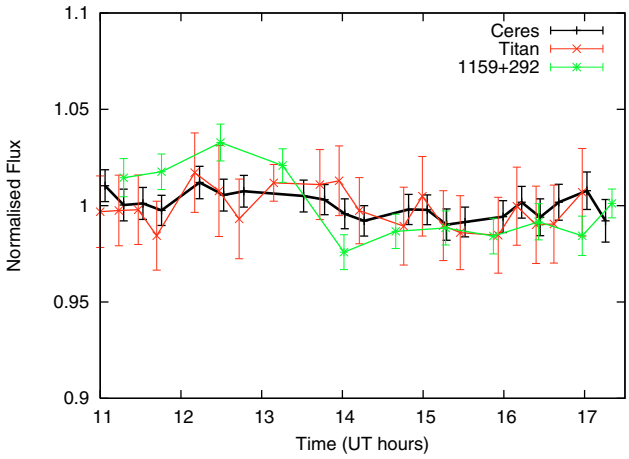

Fig. 1. Variations of Titan (red), Ceres (black) and 1159+292 flux during the track, measured on both sidebands. The plotted flux corresponds to the zero-spacing flux fit of each sub-dataset (for Titan and Ceres) or pair of sub-datasets (for 1159+292), normalized to the average flux for each source. The error bars correspond to three times the noise on the fitted data.

allowing us to retrieve the zero-spacing flux along with the sub-dataset noise σ (on the order of 10 mJy/beam). We noted that the selection of only short baselines or all baselines for this operation had little influence on the fluxes obtained, with the exception of Titan, which can show the contribution of Saturn in the beam in the shortest baselines. Projected baselines shorter than 10 m were then flagged for this source.

3. Results

Figure 1 shows that after full calibration Ceres displays flux variations of only ±1.2%, corresponding to a lightcurve amplitude of ∼2.5%. Given that the lightcurve of Titan, which is known to be flat, displays an amplitude of 3%, we can assess this value as the upper limit on the amplitude of Ceres' lightcurve. This allows us then to put an upper limit on the disk-averaged brightness temperature variation of ∼5.5 K, but the error bars make the results also consistent with a totally flat lightcurve. Assuming the variations seen are real, it appears that the hemisphere centered on 90°E would be thermally less bright than its opposite (see Fig. 2).

These results clearly disagree with the lightcurve from Chamberlain et al. (2009), because we do not see any 50% flux drop around 90°E, but they are consistent with the lightcurve at 250 GHz (Altenhoff et al. 1996) which showed only 4% amplitude variation.

The whole calibrated dataset including both sidebands has an average flux of 3.30 ± 0.02 Jy at 235.15 GHz. Taking an equivalent radius of 467.6 ± 2.2 km from Carry et al. (2008) and the mean geocentric distance at the time of observations (1.688 UA), this flux corresponds to a disk-averaged brightness temperature of 186.1 ± 6 K (taking into account both absolute and relative errors). The error on the equivalent radius assumed accounts for an additional offset error of ±1.7 K on the brightness temperature, but does not introduce any additional relative errors to the lightcurve. The obtained brightness temperature is consistent with previous measurements at similar frequencies (scaled to the same size reference): 181.5 ± 22 K at 227 GHz (Ulich et al. 1984), 176.2 ± 5.0 K at 250 GHz (Altenhoff et al. 1996). It is also the only measurement obtained with an interferometric facility, for which absolute flux calibration should be more reliable.

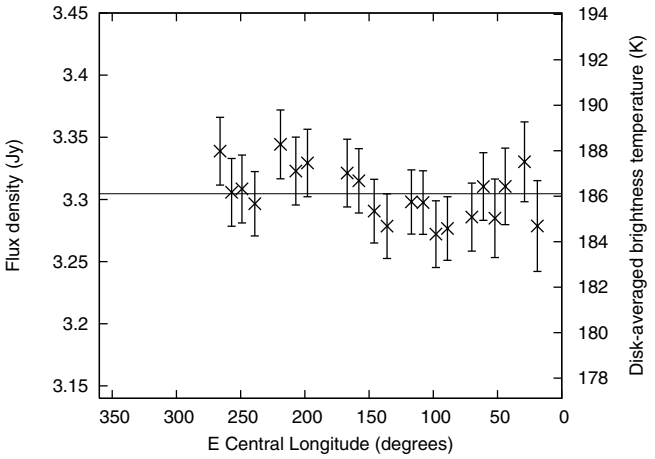

Fig. 2. Variation of Ceres' flux and corresponding disk-averaged brightness temperature as a function of the sub-earth point longitude. The plotted flux corresponds to the zero-spacing flux fit of each sub-dataset (vector averaged) at the sideband-averaged frequency of 235.15 GHz. The brightness temperature was calculated with an equivalent apparent radius for Ceres of 0.76″. Planetocentric East longitudes are reported from IMCCE ephemeris `www.imcce.fr` (Berthier 1998). The error bar corresponds to three times the noise of each sub-dataset.

4. Surface properties

The results obtained allow us to put some constraints on Ceres' surface properties. First, the 235 GHz disk-averaged brightness temperature that we measure is expected to differ from the disk-averaged surface temperature because of subsurface sounding and Fresnel refraction. This difference is characterized by the effective emissivity, i.e. the ratio of the measured brightness temperature over the expected disk-averaged surface temperature. We can estimate the ground effective emissivity at 235 GHz by calculating the expected surface temperature with a thermophysical model adapted from Spencer et al. (1989). Assuming a visible albedo value of 0.09 (Li et al. 2006) and a phase integral of 0.366 Lebofsky et al. 1986, the equilibrium subsolar temperature is 251 K for the heliocentric distance at the moment of observation (2.55 AU). With a thermal inertia of 1.5×10^4 erg cm^{-2} s$^{-0.5}$ K^{-1} (Muller et al. 1999), the expected disk-averaged surface temperature is 218 K taking into account the phase angle at the time (13°). This leads to effective emissivities in the range 0.82–0.88, including error bars. It is difficult to compare this range with previous results, because each work takes a different thermal model as reference. The value obtained only indicates that at 235 GHz the ground refractive index is lower than 4.5 (as a higher refractive index would imply a lower emissivity). It is however impossible at this point to quantify the effect of Fresnel refraction because it cannot be distinguished from the role of subsurface sounding.

The upper limit on the disk-averaged brightness temperature variation (5.5 K) constrains the distribution of a few soil properties, such as the albedo. However, the dependence of the temperature on the geometric albedo is very low ($T \propto (1 - q \times a)^{0.25}$, where a is the geometrical albedo and q is the phase integral, whose value is assumed to be 0.366 from Lebofsky et al. (1986)). If only resulting from albedo variations, a 5.5 K temperature variation would then imply high variations of disk-averaged geometric albedo (from $a = 0.$ to $a = 0.3$). Those are not expected from the latest findings, showing local albedo variations on the order of 4–6% only (Li et al. 2006; Carry et al. 2008), which would produce temperature variations of at most ∼2 K.

A variation of the ground emissivity on the order of 3% could also be invoqued. This may be the result of a variation of the refraction index by 20–25% (depending on the initial value). A variation from 0° rms to 30° rms of the characteristic roughness degree of the soil would also produce this increase in emissivity. These variations of either the roughness degree or refraction index could be physically realistic if there were an actual variation with central longitude in the composition (or nature) of the soil. As an example, water ice was measured to have a refraction index of 3.1 (Von Hippel 1954) while it can be as low as 2.5 for quartz sand (Prigent et al. 2005). The presence of variate compositions over the surface of Ceres was already suggested by Carry et al. (2008), who could assess a difference in composition between two identified terrains (bright and dark) that are inhomogeneously distributed on Ceres's surface.

These arguments prove that a thermal lightcurve amplitude of 3% could easily fit the present picture of Ceres surface. In particular, the hemisphere centered at 90°E with its large number of optically bright features (Carry et al. 2008) would have a lower disk-averaged brightness temperature than its opposite if the bright terrains had a lower emissivity than the dark ones. However, the quality of our lightcurve does not enable us to firmly assess this comparison, and then to directly relate emissivity properties to given surface features.

5. Conclusions

Using the Submillimeter Array in subcompact configuration at 235 GHz, we could obtain a 6-h long thermal rotational lightcurve of Ceres. The monitoring of different calibrators during the track enabled us to perform an accurate correction of the time-dependent gain variations, which in turn allowed us to assess that Ceres's lightcurve is flat down to a 3% level. The results obtained are incompatible with the high lightcurve amplitudes at 345 GHz reported by Chamberlain et al. (2009), but fully consistent with the lightcurve obtained at 250 GHz by Altenhoff et al. (1996), confirming the absence of very high emissivity and/or temperature variations on Ceres' disk, which would be linked to high thermophysical properties variations over large areas of the subsurface.

The ∼5.5 K upper limit obtained for the variation of disk-averaged brightness temperature could be physically reached for roughness/dielectric constant variations, which could happen if composition variations across the disk are present, as already suggested by Carry et al. (2008) from near-IR spatially resolved observations. Albedo variations could also be partially responsible for the lightcurve amplitude. Because of SNR limitations on the lightcurve, a direct comparison of the presented results to surface maps would not be meaningful, so the obtention of a complete and better measured lightcurve is necessary to relate emissivity variations to terrain features. High SNR millimeter-wave thermal maps, which could be obtained with the Atacama Large Millimeter Array (ALMA), would also allow us to constrain the emissivity (and possibly albedo) distribution, which would advance the interpretation of the expected visible and IR observations carried out by the orbiting NASA Dawn spacecraft.

Acknowledgements. We thank Mark Sykes for his helpful review of this letter, and SMA operators and staff for carrying out the observations. The Submillimeter Array is a joint project between the Smithsonian Astrophysical Observatory and the Academia Sinica Institute of Astronomy and Astrophysics and is funded by the Smithsonian Institution and the Academia Sinica.

References

Altenhoff, W. J., Baars, J. W. M., Schraml, J. B., Stumpff, P., & von Kap-Herr, A. 1996, A&A, 309, 953

Berthier, J. 1998, Notes scientifique et techniques du Bureau des longitudes, S061

Carry, B., Dumas, C., Fulchignoni, M., et al. 2008, A&A, 478, 235

Chamberlain, M. A., Sykes, M. V., & Esquerdo, G. A. 2007, Icarus, 188, 451

Chamberlain, M. A., Lovell, A. J., & Sykes, M. V. 2009, Icarus, 202, 487

Gurwell, M. A. 2004, ApJ, 616, L7

Gurwell, M. A., & Muhleman, D. O. 1995, Icarus, 117, 375

Gurwell, M. A., & Muhleman, D. O. 2000, Icarus, 145, 653

Lebofsky, L. A., Sykes, M. V., Tedesco, E. F., et al. 1986, Icarus, 68, 239

Li, J.-Y., McFadden, L. A., Parker, J. W., et al. 2006, Icarus, 182, 143

Muller, T. G., Lagerros, J. S. V., Burgdorf, M., et al. 1999, in The Universe as Seen by ISO, ed. P. Cox, & M. Kessler, ESA SP, 427, 141

Prigent, C., Munier, J., Thomas, B., & Ruffié, G. 2005, Geophys. Res. Lett., 32, 23405

Rivkin, A. S., & Volquardsen, E. L. 2010, Icarus, 206, 327

Spencer, J. R., Lebofsky, L. A., & Sykes, M. V. 1989, Icarus, 78, 337

Tedesco, E. F., Taylor, R. C., Drummond, J., et al. 1983, Icarus, 54, 23

Thomas, P. C., Parker, J. W., McFadden, L. A., et al. 2005, Nature, 437, 224

Ulich, B. L., Dickel, J. R., & de Pater, I. 1984, Icarus, 60, 590

Von Hippel, A. R. 1954, in Dielectric Materials and Applications (The Technology Press of M.I.T.)